Raman Coherence Beats from Entangled Polarization Eigenstates in InAs Quantum Dots

A. S. Lenihan,* M. V. Gurudev Dutt, and D. G. Steel†

The FOCUS Center, H.M. Randall Laboratory of Physics, The University of Michigan, Ann Arbor, Michigan 48109 and The Center for Ultrafast Optical Science, The University of Michigan, Ann Arbor, Michigan 48109

S. Ghosh and P. K. Bhattacharya

The Solid-State Electronics Laboratory, The University of Michigan, Ann Arbor, Michigan 48109

(Received 11 January 2002; published 16 May 2002)

The homodyne-detected transient four-wave-mixing response of InAs/GaAs self-assembled quantum dots shows temporal oscillations of the optically induced Raman coherence arising from two entangled polarization eigenstates of the exciton. The phase sensitive nature of the homodyne detection enables us to follow the time evolution of the nonradiative quantum coherence between the polarization states, providing a measurement of the fine-structure splitting in the dots, which is much less than the inhomogeneous broadening, and the corresponding decoherence rate of the entangled state.

DOI: 10.1103/PhysRevLett.88.223601 PACS numbers: 42.50.Md, 78.67.Hc

The interaction of coherent radiation with resonant electronic transitions leads to quantum coherence between the coupled states. For transitions in the optical region of the spectrum, the coherence is usually destroyed very quickly due to dephasing of the electronic excitation. Typically, experiments readily report on the macroscopic polarization which reflects the coherence induced between two dipole coupled states, such as that reported for self-assembled quantum dots (SAQD's) in [1,2]. However, nonradiative coherence between two states which are not dipole coupled, as in the three-level V system in Fig. 1, or the closely related Λ system, referred to as the Raman coherence, is essential for the realization of novel optical phenomena such as electromagnetically induced transparency [3,4], lasing without inversion [5–8], dark states [9–11] and the more recent work on slow light [12], and is the origin of the oscillations in luminescence observed in CdSe dots [13]. This coherence is especially important for applications to quantum logic devices [14,15] that also require coherent optical control of entangled states. Manipulation and detection of this coherence, in the dipole approximation, is nonlinear in the applied optical fields, and its detection in the time domain is enabled by detecting the time evolution of the relative phase associated with the two quantum probability amplitudes [16].

In this paper, we report the observation of the time evolution of the nonradiative Raman coherence induced between the two fine-structure split polarization eigenstates in an ensemble of SAQD's, and demonstrate the ability to optically induce and detect the resultant quantum entangled states. The quantum coherence is observed through homodyne detection of the emitted radiation arising from four-wave mixing which reports directly on the time evolution of the relative phase between the two states. The induced coherence oscillates in time after the excitation pulse with a period determined by the fine-structure splitting which is over 2 orders of magnitude smaller than the inhomogeneous broadening. The decay of the coherence and corresponding oscillation is long lived, and most likely dominated by random fluctuations in the fine-structure splitting. Physically, the coherence represents an entanglement of two distinct excitonic states, distinguished by their polarization and transition energy, similar to that reported under steady state conditions in [17] involving interface fluctuation dots. By careful choice of polarization states of the excitation and probe fields, and careful alignment with the polarization eigenaxes of the dots, we are also able to observe the polarization dependent incoherent response due to population dynamics and interstate relaxation. The measurements show the suppression of exciton spin relaxation in these structures, in agreement with earlier transient luminescence measurements [18,19].

Measurements are made on a single layer of SAQD's, formed by the Stranski-Krastenow growth mode using molecular beam epitaxy of InAs on GaAs and capped with a 100 nm layer of GaAs. From atomic force microscope images of uncapped samples, the dots are approximately hemispherical in shape, with a lateral extent of $\sim$15 nm and a height of $\sim$8 nm. The density is approximately 5×10^{10} dots/cm^2. In addition, the dots are slightly elongated along the [110] crystal axis. After growth, the sample was annealed for 30 s at 750 °C to shift the

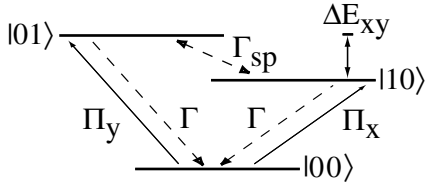

FIG. 1. Energy level diagram for an asymmetric QD. The crystal ground state is denoted by $|00\rangle$. The linearly polarized single exciton states ($|10\rangle$ and $|01\rangle$) are separated by an energy ΔE_{xy}. The exciton population decays at a rate Γ, and the relaxation rate between the polarization states is Γ_{sp}. The biexciton state ($|11\rangle$) is not excited and is not shown.

quantum dot states to higher energies. Cross-sectional scanning tunneling microscope measurements have shown that the annealing process does not lead to loss of the dot structure [20,21]. All measurements were made at 7 K.

The effects of the structural elongation of QD's have been studied both experimentally and theoretically [22–24]. For circular dots, the heavy-hole exciton states $|-1/2, +3/2\rangle$ and $|+1/2, -3/2\rangle$ are excited by circularly polarized light. However, the reduced symmetry of the confinement potential leads to mixing of the exciton spin doublet via the exchange interaction, resulting in two linearly polarized transitions which are aligned along the orthogonal in-plane axes of the dot structure. This leads to the energy level diagram shown in Fig. 1 for the ground state of the QD in the excitonic picture. Using the simpler notation for qu-bits, the crystal ground state (no excitation) is denoted by $|00\rangle$. The single exciton states, $|10\rangle$ and $|01\rangle$, have dipole transitions with polarizations labeled Π_x and Π_y, and a fine-structure splitting denoted by ΔE_{xy}. These states decay back to the ground state at a rate Γ, and relaxation between the polarization states due to spin relaxation occurs at a rate Γ_{sp}. The pulse bandwidth is small compared to the binding energy of the biexciton state $|11\rangle$ (excited by colinearly polarized fields [25]), so that excitation of the biexciton is ignored, but large compared to the hyperfine splitting.

In the measurements presented here, an optical field $\mathbf{E}_1$ is used to excite the sample. A second field $\mathbf{E}_2$, separated from $\mathbf{E}_1$ by a variable delay τ, generates a nonlinear polarization to third order in the applied fields, which in turn radiates the nonlinear signal of interest. This signal field copropagates with $\mathbf{E}_2$, and is homodyne-detected with this field on a square-law detector [16,26]. Details of this differential transmission (DT) setup can be found in [27]. The nonlinear polarization arises from distinct perturbation sequences in the density matrix picture (see, for example, [28,29]):

$$\rho_{00,00} \overset{\mathbf{E}_1(\Pi_y)}{\rightarrow} \rho_{00,01} \overset{\mathbf{E}_1^*(\Pi_y)}{\rightarrow} \begin{Bmatrix} \rho_{00,00} \\ \rho_{01,01} \\ \rho_{10,10} \end{Bmatrix} \begin{matrix} \overset{\mathbf{E}_2(\Pi_y)}{\nearrow} & \rho_{00,01} \\ & \\ \underset{\mathbf{E}_2(\Pi_x)}{\searrow} & \rho_{00,10} \end{matrix},$$

$$\rho_{00,00} \overset{\mathbf{E}_1(\sigma^{\pm})}{\rightarrow} \begin{Bmatrix} \rho_{00,10} \\ \rho_{00,01} \end{Bmatrix} \overset{\mathbf{E}_1^*(\sigma^{\pm})}{\rightarrow} \rho_{10,01} \overset{\mathbf{E}_2(\sigma^{\pm})}{\rightarrow} \begin{Bmatrix} \rho_{00,10} \\ \rho_{00,01} \end{Bmatrix},$$

where $\sigma^{\pm} = \Pi_x \pm i\Pi_y$. The term $\rho_{10,10}$ in the upper sequence is not directly excited by the optical fields because of the polarization selection rules. However, in the presence of spin relaxation, this state is coupled to $\rho_{01,01}$, and, hence, must be included at that order of the perturbation. The sensitivity in each sequence to the optical $\mathbf{E}$-field polarization gives us the ability to optically control which sequence we detect. The first sequence depends only on the population terms (diagonal matrix elements such as $\rho_{01,01}$) and the optically induced dipole. These terms are historically called incoherent since the response does not require the two optical fields to be mutually coherent. In this experimental geometry, the upper pathway of the first sequence leads, in general, to a response characterized by a decay determined by both the excited state (decay) and ground state (recovery) dynamics. The lower path is additionally sensitive to spin relaxation dynamics (between the two exciton states).

The final excitation sequence is called the coherent excitation pathway and has no contribution from population dynamics. The time evolution detected in this experimental geometry reports on the time evolution of the second order contribution $\rho_{01,10}$ [16,26] which corresponds to the excited state wave function given by $|\psi\rangle = C_{10}|10\rangle + C_{01}|01\rangle$, an entangled state involving the coherent superposition of the two different polarization eigenstates of the exciton. The oscillation in time corresponds to the energy splitting of these two states, and the decay of the oscillation corresponds to the decoherence of the superposition state. (In the experiment, it is important to note that using this polarization scheme for this perturbation sequence also leads to contributions from the previous two pathways.) Each perturbation sequence, and the corresponding dynamics, is examined experimentally.

The measurements were performed with a mode-locked Ti:sapphire laser producing pulses with an autocorrelation width of 3 ps (FWHM). Spectrally narrow ($\sim$1.4 meV) pulses were used in order to allow for selective excitation of a small part ($\sim$2.7%) of the inhomogeneous QD ensemble. The measurements were performed at low excitation, with the pump pulse creating an average density of less than one exciton per dot (the $\chi^{(3)}$ limit).

We consider first the experimental study of the first perturbation sequence which reports on the total state relaxation rate and the spin relaxation. Here, we take the field $\mathbf{E}_1$ to be Π_y. By measuring the two DT signals obtained with $\mathbf{E}_2$ having either Π_y or Π_x polarization, the relaxation back to the ground state or between the $|01\rangle$ and the $|10\rangle$ exciton states can be measured.

Figure 2(a) shows the experimental results for these two cases as the pulse delay is varied. The inset shows the spectral dependence of the nonlinear response, taken at a delay of +2 ps, showing the QD ground state resonance peaked at 1.3 eV with an inhomogeneous linewidth of $\sim$52 meV (FWHM). The transient data presented here were obtained from states at energies below the peak of the nonlinear response, to avoid known complexities associated with higher energy excitation; within these low energy states, no significant variation in the results was observed as a function of tuning. The signals shown in Fig. 2 decay on a time scale of 762.6 $\pm$ 4.5 ps, which we take to be due to exciton recombination based on comparison with earlier reports [30].

In order to best display the physics associated with polarization decay due to spin relaxation, we plot [Fig. 2(b)] the degree of linear polarization P_{Linear}, defined as $(DT_{\parallel} - DT_{\perp})/(DT_{\parallel} + DT_{\perp})$, which is sensitive to the relaxation of the optical orientation. We observe a two part decay; after the fast initial decrease of the polarization, the remaining optical orientation decays extremely slowly. Fitting the data to a biexponential curve yields decay times of

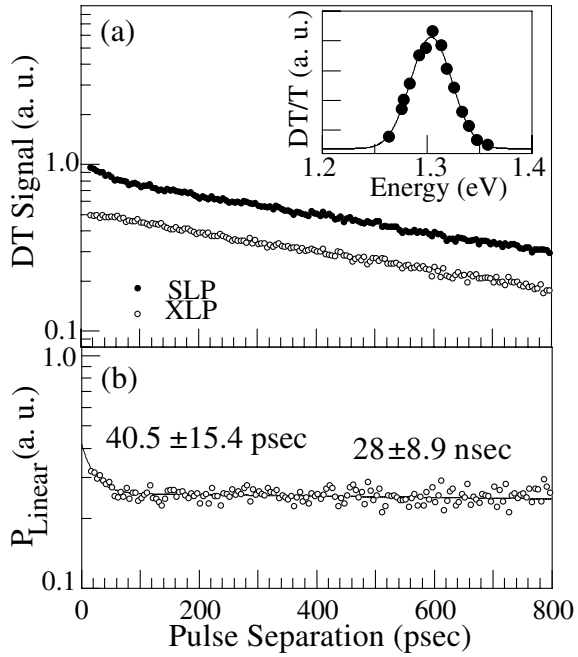

FIG. 2. (a) Polarization dependent transient nonlinear optical response of InAs dots. The excitation fields are polarized along the QD axes, with field $\mathbf{E}_2$ polarized parallel (SLP) or perpendicular (XLP) to field $\mathbf{E}_1$. The inset shows the nonlinear optical spectrum of the QD ground state, taken at a small positive delay. (b) The linear polarization (as defined in text) derived from the curves in (a). After an initial drop, the polarization relaxes slowly, indicating a suppression of exciton spin flip processes. A biexponential fit (solid line) yields time scales of 40.5 ± 15.4 ps and 28 ± 8.9 ns for the two decay components.

40.5 ± 15.4 ps and 28 ± 8.9 ns for the two components. The slow component is indicative of the slow relaxation of the exciton spin in these QD's, as compared to higher dimensional structures [31,32] and confirms earlier reports for similar systems [18,19].

The biexponential decay, which was not observed in [18,19], is not predicted by the simple model considered here and may simply be indicative of heterogeneity within the dot ensemble, wherein some dots undergo rapid spin relaxation. However, it may be that the above model for relaxation is incomplete and that more sophisticated models, such as those which include the presence of dark states and lead to more complex decay dynamics [33], may be more appropriate. Unfortunately, the many free parameters included make quantitative comparisons with the data less reliable and will require single QD studies.

We now consider the special case where circular polarized fields simultaneously excite both the $|01\rangle$ and $|10\rangle$ exciton states, identified in the final perturbation sequence. This leads to a coherent superposition for the excited state wave function of the form $|\psi_{ex}\rangle = C_{10}|10\rangle + C_{01}|01\rangle$, represented by the density matrix element $\rho_{10,01}$. Clearly, this experiment includes the previous physical features, but also includes the new features associated with the last perturbation sequence. Because of the use of the phase sensitive technique, the temporal evolution of $\rho_{10,01}$ can be observed and manifests itself as oscillations at the energy splitting, ΔE_{xy} (Fig. 1), in the time domain [16,26].

Figure 3(a) shows the oscillation of the Raman coherence for $\mathbf{E}_1$ and $\mathbf{E}_2$ having circular polarizations of either the same (SCP) or opposite (OCP) helicity, chosen to coherently excite both polarization eigenstates. Similar results are, of course, found for linearly polarized fields oriented 45° relative to the polarization axes of the dots. A clear oscillatory signal is observed superimposed on the signal resulting from the incoherent population decay. As anticipated in [34], the oscillations observed in the cases of SCP and OCP fields show a phase shift of π relative to one another. The observation of beats in the homodyne-detected geometry immediately yields the first direct evidence of an optically created coherent nonradiative superposition in these systems.

Figure 3(b) shows the theoretical analysis based on solutions of the density matrix equations following the perturbation sequences outlined above for parameters appropriate for this experiment. The theoretical picture, similar to that in [26], confirms not only the phase shift for the two different polarization configurations, but also shows that, in the absence of the last perturbation sequence above, there are no beats in the homodyne-detected geometry [16].

By subtracting the two curves in Fig. 3, it is possible to isolate the coherent response from the overall population decay, as shown in the inset. Because this is an ensemble measurement, the signal is the average of the response of many dots, each with potentially different exchange energy splittings. This is most likely the origin of the observed damping of the quantum beats rather than intrinsic decoherence. In the language of NMR, this is referred to as T_2^*

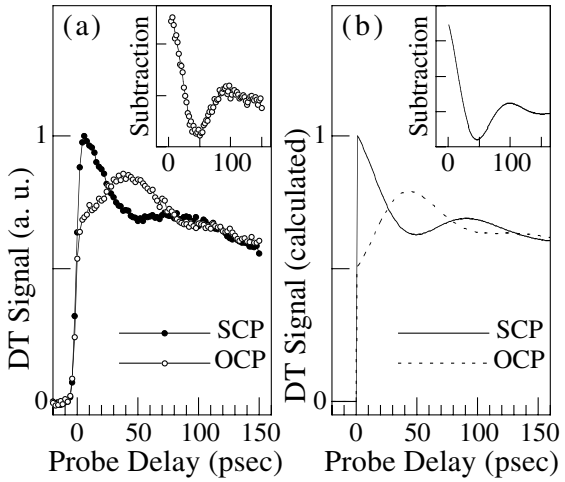

FIG. 3. (a) Raman coherence beats observed in the transient nonlinear response, with circularly polarized fields. The cases of the optical fields having the same (SCP) and opposite (OCP) circular polarizations are shown, leading to the expected π phase shift in the oscillations. Inset: Subtraction of the two data curves shows the isolated coherent contribution. The beat period of 102.35 ± 2.92 ps corresponds to a fine-structure splitting of 40.35 μeV. (b) Calculated total nonlinear response.

and follows from averaging the polarization over an inhomogeneous distribution of fine-structure splittings. Hence, this ensemble measurement cannot directly measure the true homogeneous coherence time of the nonradiative coherent superposition state.

From the data, we note that the oscillation period of 102.35 ± 2.92 ps yields an average fine-structure splitting $\Delta E_{xy} = \hbar(\omega_y - \omega_x)$ of ~ 40.35 μeV, slightly smaller than that reported in single dot measurements [23]. The damping of the oscillations has an effective decay time of order 58.46 ± 1.45 ps, corresponding to the inhomogeneous distribution of energy splittings. Effective decay times of up to 80 ps have been observed in this sample, and, hence, set the lower limit on the homogeneous nonradiative Raman coherence time, T_2, which is already significantly longer than that observed in bulk GaAs in similar measurements [26], and that inferred from frequency-domain measurements in interface fluctuation QD's [17]. Measurements to establish the real T_2 will most easily be accomplished by repeating this kind of experiment on single quantum dots.

Finally, as given above, the observed oscillations arise from the energy difference of the two states of the excited state wave function, $|\psi_{ex}\rangle = C_{10}|10\rangle + C_{01}|01\rangle$. The complete state is given by $|\psi\rangle = C_{00}|00\rangle + C_{10}|10\rangle + C_{01}|01\rangle$. This is a nonfactorizable state because the biexciton state was out of resonance and not excited. The dephasing rate that we measure is therefore the decoherence of this entangled state and demonstrates that these systems represent a potential basis for quantum computing devices and quantum information applications [14,15]. An essential requirement to complete the extension of this system to a simple two qu-bit device, of course, requires the direct excitation and control of the biexciton state, corresponding to $|11\rangle$. This has now been achieved in hole burning experiments [25].

This work was supported in part by the U.S. ARO (DAAD19-99-1-0198), by the NSA and ARDA (ARO Grant No. DAAG55-98-1-0373), by AFOSR (F49620-99-1-0045), and by the NSF (STC-PHY-8920108).

*Present address: The Laboratory for Physical Sciences, College Park, MD 20740.

†Electronic address: dst@umich.edu

[1] P. Borri *et al.,* Phys. Rev. Lett. **87**, 157401 (2001).
[2] D. Birkedal, K. Leosson, and J. M. Hvam, Phys. Rev. Lett. **87**, 227401 (2001).
[3] K. J. Boller, A. Imamoglu, and S. E. Harris, Phys. Rev. Lett. **66**, 2593 (1991).
[4] J. E. Field, K. H. Hahn, and S. E. Harris, Phys. Rev. Lett. **67**, 3062 (1991).
[5] S. E. Harris, Phys. Rev. Lett. **62**, 1033 (1989).
[6] M. O. Scully, S. Y. Zhu, and A. Gavrielides, Phys. Rev. Lett. **62**, 2813 (1989).
[7] M. O. Scully, Quantum Opt. **6**, 203 (1994).
[8] O. A. Kocharovskaya and Y. I. Khanin, Sov. Phys. JETP **63**, 945 (1986).
[9] E. Arimondo and G. Orriols, Nuovo Cimento Lett. **17**, 333 (1976).
[10] R. M. Whitley and C. R. Stroud, Jr., Phys. Rev. A **14**, 1498 (1976).
[11] M. Lindberg and R. Binder, Phys. Rev. Lett. **75**, 1403 (1995).
[12] L. V. Hau *et al.,* Nature (London) **397**, 594 (1999).
[13] T. Flissikowski *et al.,* Phys. Rev. Lett. **86**, 3172 (2001).
[14] E. Biolatti *et al.,* Phys. Rev. Lett. **85**, 5647 (2000).
[15] P. C. Chen, C. Piermarocchi, and L. J. Sham, Phys. Rev. Lett. **87**, 067401 (2001).
[16] R. Binder *et al.,* Phys. Status Solidi (b) **221**, 169 (2000).
[17] G. Chen *et al.,* Science **289**, 1906 (2000).
[18] H. Gotoh *et al.,* Appl. Phys. Lett. **72**, 1341 (1998).
[19] M. Paillard *et al.,* Phys. Rev. Lett. **86**, 1634 (2001).
[20] B. Lita *et al.,* Surf. Rev. Lett. **7**, 539 (2000).
[21] B. Lita and R. S. Goldman (unpublished).
[22] D. Gammon *et al.,* Phys. Rev. Lett. **76**, 3005 (1996).
[23] M. Bayer *et al.,* Phys. Rev. Lett. **82**, 1748 (1999).
[24] T. Takagahara, Phys. Rev. B **62**, 16 840 (2000).
[25] A. S. Lenihan *et al.* (to be published).
[26] K. B. Ferrio and D. G. Steel, Phys. Rev. Lett. **80**, 786 (1998).
[27] J. Shah, *Ultrafast Spectroscopy of Semiconductors and Semiconductor Nanostructures* (Springer-Verlag, Berlin, 1996), 1st ed.
[28] I. M. Beterov and V. P. Chebotaev, Prog. Quantum Electron. **3**, 1 (1974).
[29] M. O. Scully and M. S. Zubairy, *Quantum Optics* (Cambridge University Press, Cambridge, England, 1997).
[30] M. Paillard *et al.,* Appl. Phys. Lett. **76**, 76 (2000).
[31] T. C. Damen *et al.,* Appl. Phys. Lett. **58**, 1902 (1991).
[32] L. Muñoz *et al.,* Phys. Rev. B **51**, 4247 (1995).
[33] M. Z. Maialle, E. A. de Andrada e Silve, and L. J. Sham, Phys. Rev. B **47**, 15 776 (1993).
[34] S. Schmitt-Rink *et al.,* Phys. Rev. B **46**, 10 460 (1992).